J. Anat. (1977), **124**, 3, pp. 563–580
With 20 figures
Printed in Great Britain

Facial and visceral arch development in the mouse embryo: a study by scanning electron microscopy

ARNOLD TAMARIN* AND ALAN BOYDE

Department of Anatomy and Embryology, University College London, Gower Street, London, WC1E 6BT

(*Accepted* 19 *August* 1976)

INTRODUCTION

Much of what is known about facial morphogenesis in mammals is based on the study of human embryos (Streeter, 1942, 1948; Cadenat, 1961), and rather few studies have been devoted exclusively to the detailed development of external facial features in rodents (Grüneberg, 1943; Otis & Brent, 1959; Christie, 1964). The basic pattern of facial development is similar in all mammals, and there is little disagreement over fundamentals. However, the origin and fate of the visceral arches have been the subject of intermittent controversy among comparative anatomists and embryologists ever since theories concerning the segmental origin of the vertebrate head were proposed in the first half of the nineteenth century (Owen, 1848). As suggested by Sudler (1902), early enthusiasm for this subject was generated, in part, by the quest for 'proof' of Haeckel's biogenetic principle of recapitulation; as a consequence much of the original data concerning visceral arch development arose out of studies of head segmentation in elasmobranchs (Balfour, 1878; Locy, 1895; Goodrich, 1918).

Although some aspects of the head segmentation problem remain unresolved (Wedin, 1954), the idea that visceral arches are a manifestation of primary somitic metamerism was long ago refuted by Kingsbury (1926), and is no longer a contested issue. (For a terse account of the polemics concerning head segmentation and branchiomerism, see Nelsen, 1953).

More recently, studies of the face and visceral arches have been concerned with cytological aspects of the relationship between embryonic and postnatal structures (Barry, 1961). But, curiously, standard contemporary descriptions of the overall external aspect of the mammalian branchial region appear to be based on studies published prior to 1927, particularly those of His (1886) and of Frazer (1926).

The advent of scanning electron microscopy, and the development of techniques for drying tissue without significant distortion of surface structure, has made it possible to re-examine the morphology of embryos at a resolution which is about 1000 times better than that obtained using conventional incident-light optical methods (Waterman, 1974*a*, *b*; Watson *et al.* 1976).

Although many investigators have applied scanning electron microscopy to the study of embryological topics (see bibliographies provided by Boyde, Jones & Bailey, 1973; Jones, Bailey & Boyde, 1974; Johnson, 1976) no authors have specifically concerned themselves with the morphogenesis of the visceral arch complex in mammals.

* Department of Oral Biology and Department of Biological Structure, University of Washington, Seattle, WA, 98195, U.S.A. Visiting Investigator, University College London, 1975–76.

In the light of the ubiquitous use of mice for embryological experimentation it would seem desirable to have as complete a record as possible of the surface topography of normal development in this animal. The purpose of this report is to give an account of the normal development of the face and exterior visceral arch region in the mouse embryo as visualized by scanning electron microscopy, in order to provide a more precise basis for experimental studies of facial and cervical morphogenesis.

The term 'visceral arch' in this report refers to the mandibular arch (I), the hyoid arch (II) and all succeeding arches. The term 'branchial arch' refers only to those which are phylogenetically homologous with the gill arches of lower vertebrates, and thus I and II are excluded (Nelsen, 1953). In this paper, visceral arches are designated by roman numerals I, II, III, IV, and visceral grooves by arabic numerals G-1, G-2, G-3, G-4.

METHODS AND MATERIALS

This report is based on the study of embryos taken from 14 randomly bred mice of the CD-1 strain. Dams were killed by swift cervical dislocation at 8·3 days *post coitum* and thereafter at 24 hour intervals up to and including day 13. There was a total of 119 embryos; of these, 16 were discarded as being obviously abnormal or ruined during their dissection from enveloping membranes, and another 40 were judged unusable because of imperfections acquired during processing for scanning electron microscopy. The data presented were from 63 embryos, comprising at least 6 embryos from each time period.

Conceptuses were removed from excised whole uteri and submerged in isothermal normal saline solution, using a modified form of the procedure described by Kirby (1971). Embryos were then freed from their extra-embryonic membranes with fine pointed forceps under a dissecting microscope and put into 3% glutaraldehyde in 0·2 M cacodylate buffer for 16–20 hours. At this point some of the embryos were cut with razor blades so as to separate the head plus branchial region from the heart bulge in order to provide an unobstructed view of the face in the scanning electron microscope. All the specimens were repeatedly rinsed in buffer solution and then immersed in 3% OsO_4 in cacodylate buffer for 16–20 hours, after which they were thoroughly rinsed in distilled water. The smallest specimens (8 and 9 day embryos) were then transferred by pipette to small lens-paper bags to facilitate handling during subsequent drying procedures. All specimens were dehydrated through graded ethanol solutions over 5–6 hours, ending with two changes in anhydrous alcohol.

Fig. 1. (stereo). *PW* = 0·45 mm. Stage 12, early; fronto-lateral aspect of brain-plate. Prosencephalon (*P*) is flaired laterally and the primary optic vesicles (*V*) form concavities on the anterior surface. *G*, foregut antrum; *H*, heart bulge; M, mesencephalon; *E*, encephalic groove.

Fig. 2. *PW* = 0·80 mm. Stage 12, late; posterior–lateral aspect of brain-plate. Brain segments are more distinct and the cervical fold (*c*) has formed. *M*, mesencephalon; *Mt*, metencephalon; *My*, myelencephalon; *A*, amnion; *Co*, intra-embryonic coelom.

Fig. 3. *PW* = 0·70 mm. Stage 13, early; lateral aspect of head region. Mandibular arch (I) has appeared between fore-brain (*P*) and heart bulge (*H*). The first visceral groove (*G-1*) appears as the continuation of the groove separating the mid-brain (*M*) from the metencephalon (*Mt*). The cervical fold (*C*) extends perpendicularly from the metencephalon toward the amnion (*A*).

Fig. 4. *PW* = 0·95 mm. Stage 14; latero-frontal aspect of head region. *R*, mid-sagittal ridge; *F*, bulges of frontal prominence; *S*, stomatodeum; *H*, heart bulge area.

Fig. 5. *PW* = 0·50 mm. Stage 14; lateral aspect of neck region. Postmandibular area contains primordia of hyoid arch (II), arch III and interarch grooves *G-1*, *G-2* and *G-3*. The otic placode (*O*) has a slightly concave surface.

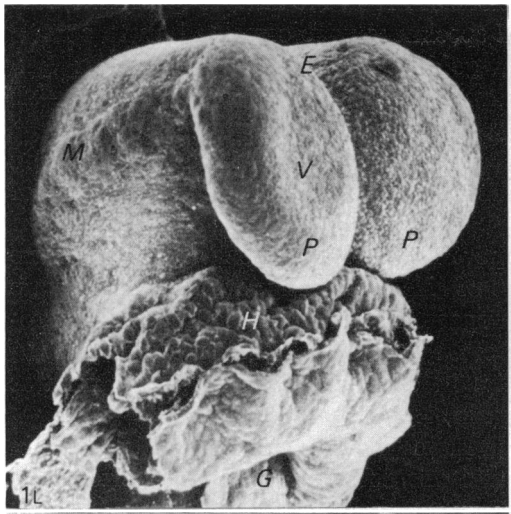
E
M
V
P
P
H
G
1L

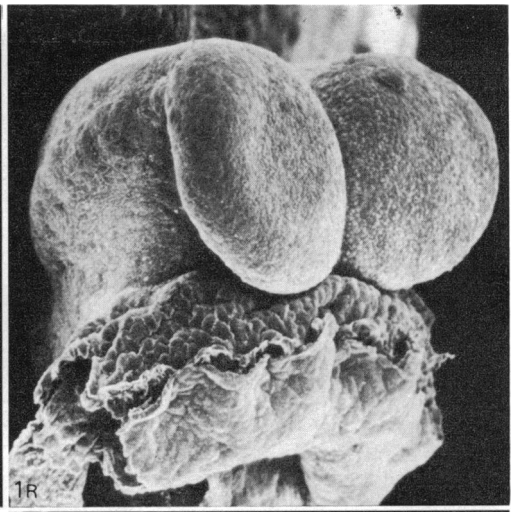
1R

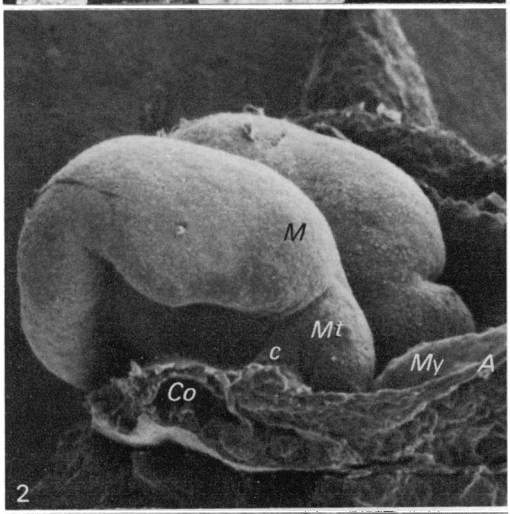
M
Mt
c
My
A
Co
2

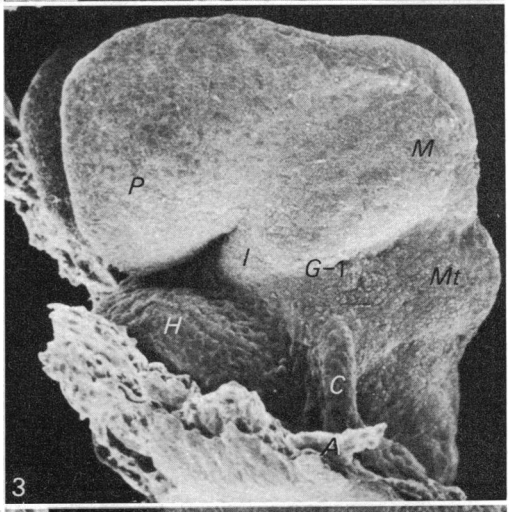
M
P
I
G-1
Mt
H
C
A
3

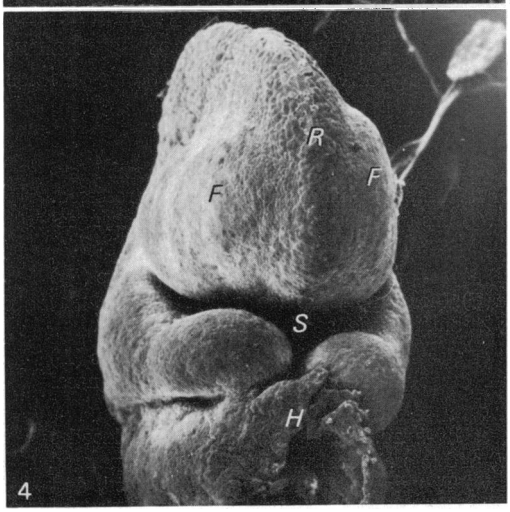
R
F
F
S
H
4

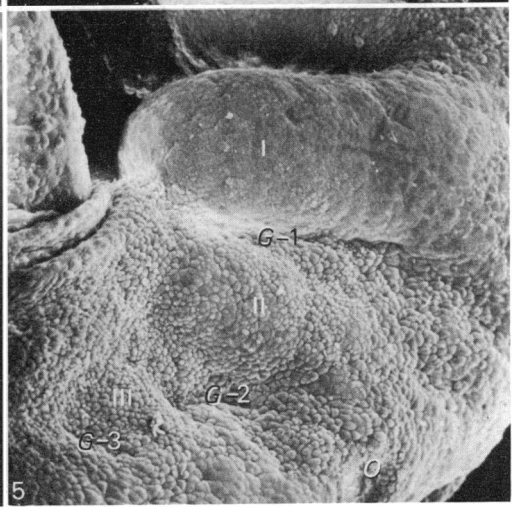
I
G-1
II
III
G-2
G-3
C
5

The alcohol was substituted in graded solutions of Freon-113 and the specimens were critical-point dried in a CO_2 bomb. Dried specimens were cemented on to convex aluminium stubs and sputter-coated with gold in an argon atmosphere at 0·15 Torr for a total of 3 minutes using a sequence of 15 second, 20 mA, 1·2 kV, on–off bursts to avoid overheating.

Micrographs were taken with a Cambridge-Stereoscan S4-10 at 10 kV using apertures of 50, 100 or 200 μm. Stereo-pairs were taken at a tilt-angle difference of 10 degrees.

The measurements provided in this report have no statistical validity and are meant to serve merely as rough indicators of size and change with time: they are not compensated for shrinkage during preparation for scanning electron microscopy. Waterman (1974*b*) suggests that embryonic tissue suffers about a 27% linear reduction during processing: studies in our own laboratory confirm this (about 32%, Boyde, Bailey, Jones & Tamarin, 1977).

The magnification of illustrations are given as 'picture width' (*PW*) because, in scanning electron microscope pictures, actual size differs from apparent size in the third dimension.

OBSERVATIONS

Murine embryos exhibit different degrees of development within the same litter (Burlinghame & Long, 1939) and thus it is possible to arrange the specimens in a sequence of increasing morphological maturation. In this study the most mature specimens of one chronological group were as highly developed as (or more developed than) the least mature specimens of the next older chronological group. Thus the final collection of specimens represented a fairly close sequence of stages throughout the *embryonic* period of development.

Authors differ in their chronologies of mouse development (Grüneberg, 1943; Otis & Brent, 1959; Rugh, 1968; Theiler, 1971). In this study Theiler's (1971) stages were used as the basis for recording the progress of development.

Stage 12, *early* (*Fig.* 1)

At this stage (early on the eighth day) the mouse embryo has not yet undergone flexion or rotation and the dorsum is concave at the bottom of the egg cylinder. The head primordia are dominated by the flattened anterior wings of the prosencephalon, which flare laterally on either side of the encephalic groove. The primary optic vesicles

---

Fig. 6 (stereo). *PW* = 1·5 mm and Fig. 7, *PW* = 0·85 mm. Stage 15; lateral aspect of head. Maxillary process (*X*) forms as lateral bulge at base of I. Entire postmandibular arch area is recessed. Arch IV and *G-4* have developed. Otic placode (*O*) has invaginated and the glossopharyngeal placode (*G*) has formed. A magnified view of the visceral arch region is provided in Fig. 7.

Fig. 8. *PW* = 2·0 mm. Stage 16; frontal (ventral) aspect of whole embryo. Frontal groove (*Fg*) has formed between bulges of frontal prominence (*F*). Incipient nasal placode (*N*) is flat. *H*, heart bulge; *L*, fore-limb bud; *U*, umbilical complex; *A*, amnion; *So*, somites; *T*, tail region.

Fig. 9. *PW* = 0·60 mm. Stage 16; lateral aspect of visceral arch region. Maxillary process (*X*) extends above commissure (*C*) of stomatodeum. Optic placode (*Op*) is elevated whilst nasal placode (*N*) is flat. *S*, cervical sinus.

Fig. 10. *PW* = 1·6 mm. Stage 17; lateral aspect of head. Nasal (*N*) and optic placodes are invaginated. The medial nasal process (*MN*) and lateral nasal process (*LN*) are separated above the nasal antrum by a constriction (arrow). The cervical sinus region is reduced, and III is partly tucked under II. The vestige of IV remains as a tag below the epipericardial ridge (*R*).

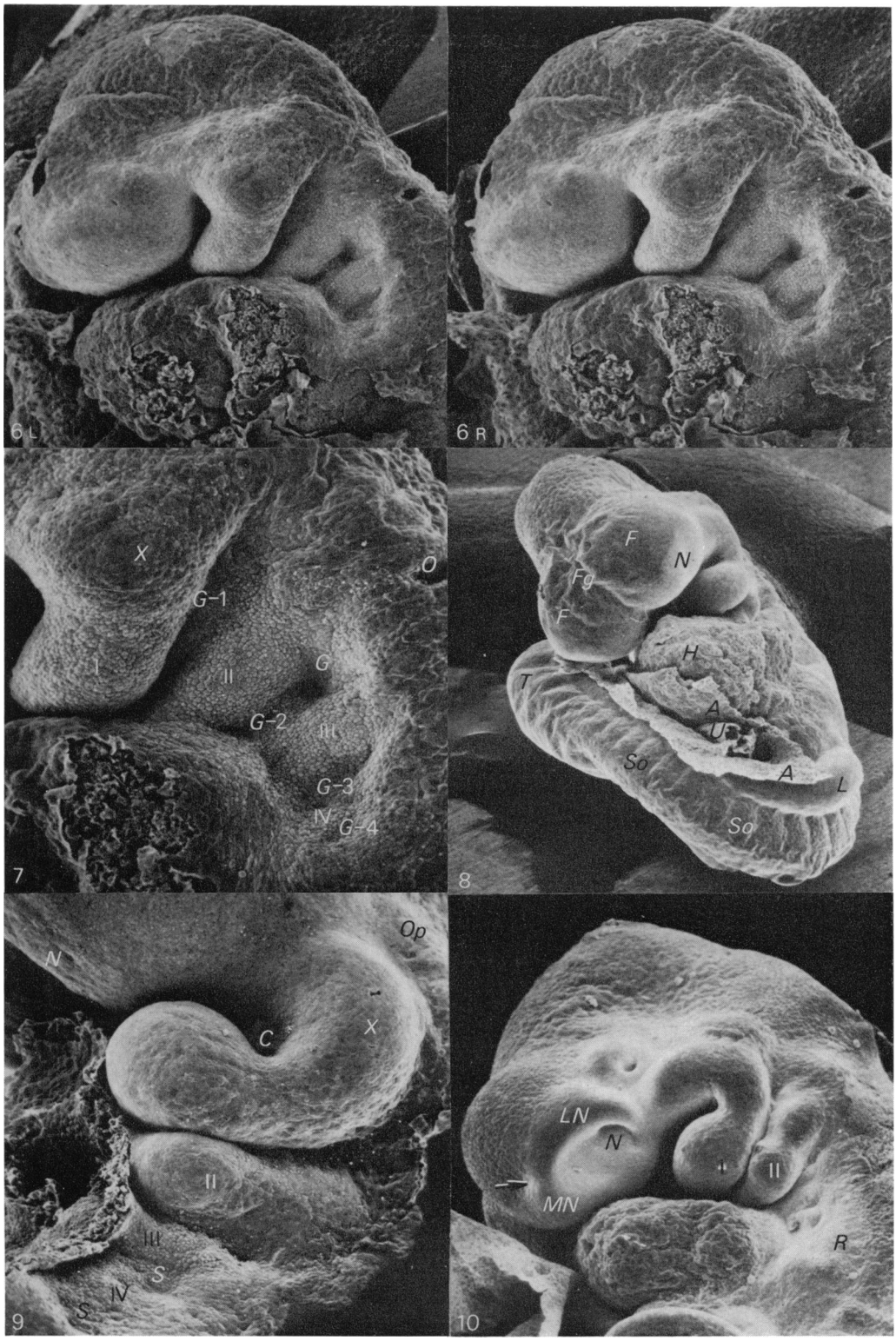
6 L
6 R
X
O
G–1
I
II
G
G–2
III
G–3
IV
G–4
7
F
N
Fg
F
H
T
A
U
So
A
L
So
8
Op
N
C
X
II
III
S
IV
S
9
LN
N
II
MN
R
10

appear as incipient concavities on the anterior surface (these will establish the base of the diencephalic ventricle when convergence and fusion of the cephalic folds occur).

The future oral antrum and branchial region will begin to develop within the region bounded in front by the deep surface of the overhanging flaired forebrain; below, by the upper surface of the heart bulge; above and behind, by the front of the mid- and hind-brain (this region is about 0·19 mm long and 0·14 mm wide).

Stage 12, *late* (*Fig.* 2)

At this stage (about the middle of the eighth day) the mid-brain has elongated. A buttress-like structure (the cervical fold) extends laterally from the anterior–inferior aspect of the hind-brain, just caudal to the isthmus, and merges with the somatopleure above the septum transversum at the posterior region of the heart primordium.

The cephalic flexure has begun to form and now the region of future visceral arch development assumes a rectangular shape which is bounded anteriorly by the telencephalon; superiorly, by the diencephalon and mesencephalon; inferiorly, by the heart bulge and, posteriorly, by the cervical fold.

Stage 13, *early* (*Fig.* 3)

Just prior to rotation and subsequent reversal of the embryonic curvature the fore-brain makes a right angle with the hind-brain as the result of continued cephalic flexion. The first visceral arch (mandibular, I) now becomes discernible as a slight bulge anterior to the inferior part of the mid-brain. It is about 0·08 mm wide and projects about 0·01 mm forward and downward into the stomatodeal depression between the fore-brain and the heart bulge. The first visceral groove (G-1) is shallow and appears to continue dorsally as the sulcus between the mesencephalon and metencephalon.

The cervical fold is now enlarged ($\sim$ 0·04 mm thick) and extends outward and backward from the inferior–lateral surface of the hind-brain. At this stage, the heart bulge and the region of visceral arch formation appear to lie within a 0·35 by 0·2 mm subcompartment of the amniotic space. It is bounded anteriorly by the procephalic membrane, superiorly by the inferior aspect of the fore- and mid-brain, ventrally by the pericardial somatopleure, laterally by the amnion, and posteriorly by the cervical fold.

Fig. 11. (stereo). *PW* = 2·0 mm. Stage 18; fronto-lateral aspect of head. Wide frontal groove (*F*) extends into stomatodeum (*St*). There is a marked enlargement of the nasal processes, the maxillary process and the prebranchial arches (I and II). Cervical sinus is recessed area beneath II. Arrow, lambdoid junction.

Fig. 12. (stereo). *PW* = 2·0 mm. Stage 18; lateral aspect of the same specimen seen in Fig. 11. Globular process (*G*) of medial nasal process extends below antrum of nasal canal and the groove between the maxillary (*X*) and lateral nasal process (*LN*) has deepened. Note the vagus placode elevation in the cervical sinus (*S*).

Fig. 13. *PW* = 2·5 mm. Stage 19; frontal–inferior aspect of face. The frontal groove has narrowed (compare with Fig. 11) and the primary choanae (arrow) are present. The maxillary process (*X*) has more contact with the lateral nasal process (*LN*) than with the medial nasal process (*MN*).

Fig. 14. *PW* = 2·3 mm. Stage 19; fronto-lateral aspect of head. External auditory meatus (arrow) is beginning to form and the vagus placode is deeply invaginated in the cervical sinus (*S*).

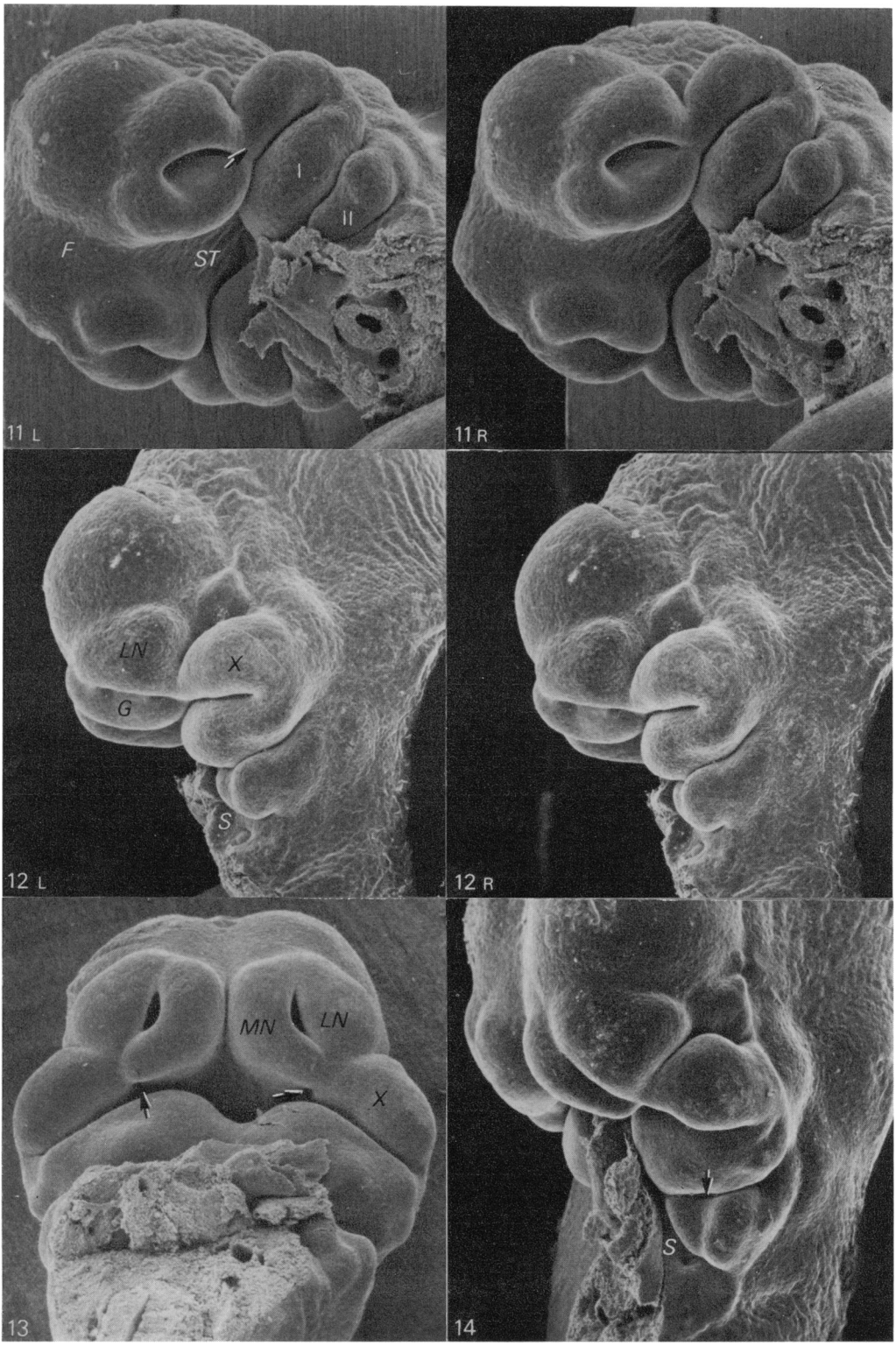
I
II
F
ST
11 L
11 R
LN
X
G
S
12 L
12 R
MN
LN
X
13
S
14

Stage 14 (*Figs.* 4 *and* 5)

At this stage, at the beginning of the ninth day, after the embryo has rotated but before flexion is completed, the encephalic groove is completely filled in. The widest part of the embryo (0·54 mm) is at the base of the mandibular arches (i.e. below the commissural angles of the stomatodeum). This is about 0·1 mm more than the width across the frontal prominence. The latter shows lateral bulges on either side of the midsagittal ridge formed by the fusion of the right and left brain primordia. Developing nasal placodes appear as slightly flattened areas on the sides of the frontal prominence but, as yet, there are no distinct indications of nasal processes.

The anterior part of arch I has doubled in thickness (0·16 mm) and has elongated about 7·5-fold (0·3 mm) in a ventral direction between the frontal prominence and the heart bulge. However, the lower border of the stomatodeum is incomplete, because the rounded extremities of the right and left arches are still about 0·03 mm apart.

The visceral arch region caudal to I has expanded to become a triangular area (about 0·36 mm long) in which the hyoid arch (II) has appeared as an elongated (0·23 mm) elevation parallel to I. It is clearly demarcated from I by a shallow groove (G-1) which is about 0·05 mm wide dorsally, narrowing ventrally where the surface of II merges with the pericardium. Just anterior to the otic placode, the base of II is confluent with the hind-brain prominence.

The cervical sinus has formed as a depressed triangular area caudal to II. This region has a steep inclination toward the otic placode dorsally, but inclines gradually towards the heart bulge ventrally. A slight convexity (0·05 mm wide) rises from the floor of the depression to form the primordium of III. The space (G-2) between II and III is about 0·05 mm wide and has a flat floor, except dorsally where an indentation marks the glossopharyngeal placode. Posterior to III, a dimple-like depression in the cervical sinus marks the site of G-3. Its caudal boundary is the epipericardial ridge which appears to have originated from the cervical fold of the prerotation embryo.

Fig. 15. *PW* = 2·7 mm. Stage 20; lateral aspect of head. Nasal area has developed snout-like profile. External auditory meatus (*A*) has widened and the facial nerve placode (arrow) can be seen in *G-1*. Tubercles on I and II are well developed. Cervical sinus is the small triangle between the abdominal bulge (*B*) and the epipericardial ridge (*R*).

Fig. 16. *PW* = 1·9 mm. Stage 20; ventro-lateral aspect of stomatodeum and visceral arch region of same specimen seen in Fig. 15. Upper lip outline is developing mature secondary undulations. The union of maxillary (*X*) and lateral nasal process (*LN*) has increased in width. *A*, auditory meatus; arrow, facial nerve placode; *S*, cervical sinus.

Fig. 17. *PW* = 4·2 mm. Stage 21; fronto-lateral aspect of head and abdominal region. Frontal groove (*G*) has become a shallow depression. Medial border of maxillary process seen as faint depression (arrow) whilst other grooves are all but obliterated. External nares have inverted comma shape. Supra-orbital tubercles (*T*) have formed. Antrum of auditory meatus has enlarged and become round in outline. Note the placodes of maxillary vibrissae.

Fig. 18. *PW* = 0·03 mm. Epithelial cells of pebbly surfaces (see Figs. 5, 7 and 8) are rounded and have randomly distributed microvilli.

Fig. 19. *PW* = 0·03 mm. Epithelium of intermediate surface texture. Cells are flattened and have microvilli over their whole surface but concentrated near cell boundaries.

Fig. 20. *PW* = 0·05 mm. Epithelial cells of smooth areas. Microvilli are restricted to the boundaries of these flat cells

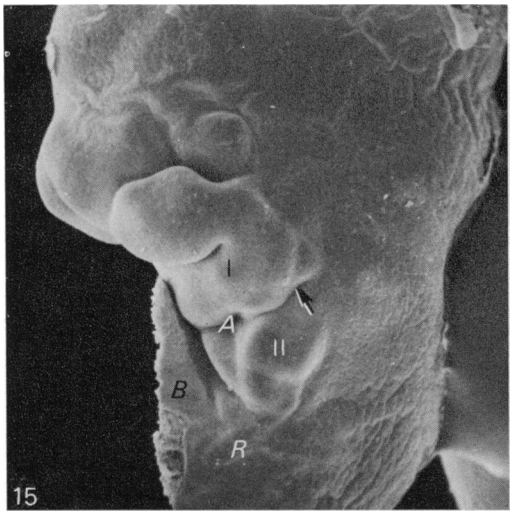

15

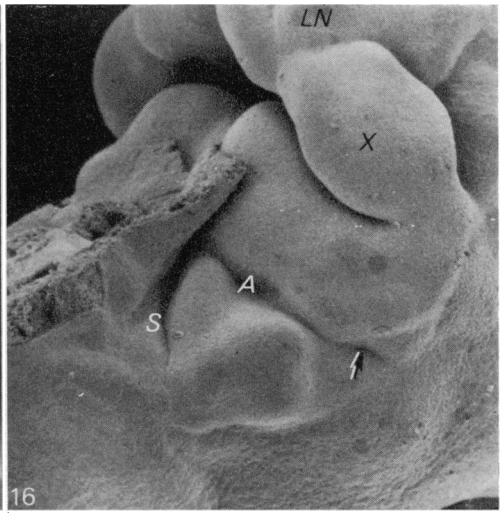

16

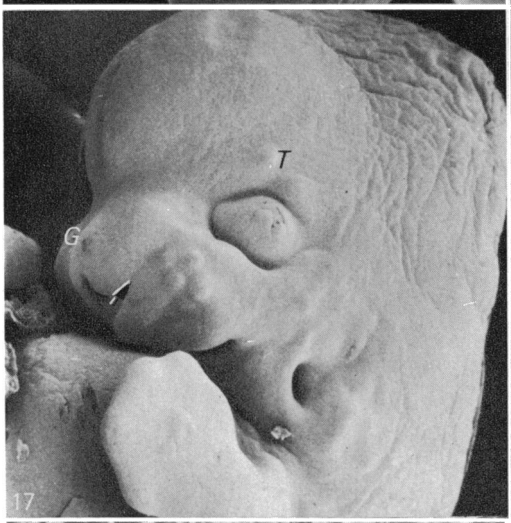

17


18

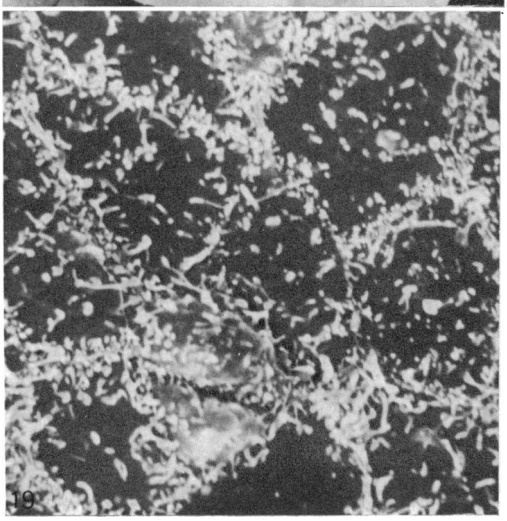
19

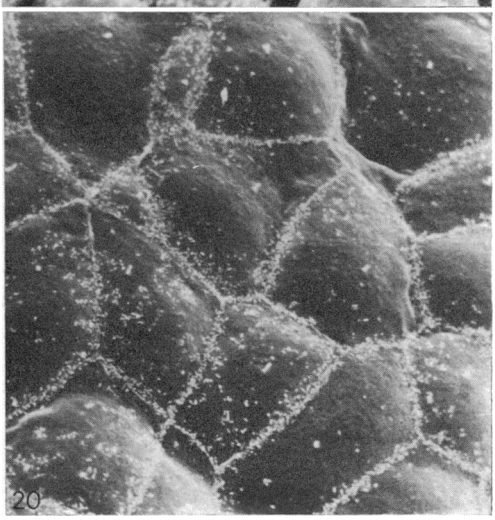
20

Stage 15 (*Figs.* 6 *and* 7)

At this stage (around nine and a half days) the frontal prominence is smooth as a result of the disappearance of the midsagittal ridge and the enlargement of the lateral bulges. The base of I has widened (0·36 mm) cranio-caudally and has developed a lateral bulge representing the origin of the maxillary process. The central region of I, which has also widened (0·22 mm), now curves toward the upper frontal margin of the stomatodeum, thereby creating an angle at the maxillary bulge below and medial to the commissure.

The entire visceral arch region posterior to I is recessed as the result of differential expansion of the surrounding structures, i.e. I anteriorly, the heart bulge ventrally, the epiricardial ridge posteriorly and the hind-brain prominence dorsally.

Actually, arch II has also enlarged (0·28 mm long, 0·15 mm wide) and appears more distinct because of the deepening of G-1 and G-2. The floor of G-2 is no longer flat and the glossopharyngeal placode has sunk to form a pit. The otic placode directly above G-2, near the dorsum of the hind-brain, has also invaginated.

The cervical sinus is larger, III has expanded (0·19 mm long, 0·11 mm wide) and G-3 is deeper and longer. But the most notable change is the addition of IV and G-4 within the distal angle of the sinus, where they closely resemble III and G-3 at the previous developmental stage.

Stage 16 (*Figs.* 8 *and* 9)

At this stage (about 10 days) the two bulges of the frontal prominence have expanded forward and laterally so that a midsagittal depression (frontal groove) is formed at the site of the sagittal ridge of earlier stages. It is formed in the centre of the lower half of the head and extends into the antrum of the stomatodeum. The nasal placode areas are now slightly concave, so that the lower part of each bulge is divided into a medial and lateral portion (nasal processes).

The maxillary bulge of I has expanded laterally and superiorly around, and above, the stomatodeal commissure. It is separated from the lateral nasal process by a shallow depression. Dorsal to this depression, in the angle formed between the lateral nasal and maxillary processes, the optic placode appears as a slight elevation.

The ventral (medial) part of I has expanded more than the middle part (adjacent to the maxillary bulge) so that, from the side, the stomatodeal commissure is curved downward.

Arch II extends almost as far ventrally as I: at its ventro-lateral angle there is a knob-like prominence which touches I across G-1 and then curves medially to merge with the pericardium.

The growth of structures within the cervical sinus is retarded as compared with I and II. Although III is still fairly prominent, the contour of IV is reduced, so that the entire region occupied by G-3, IV and G-4 is now a single flat-bottomed depression.

At this stage of development, and to a lesser extent at the previous stage, changes occur in the surface of the epithelium. It will be seen in Figures 7 and 9 that the surfaces of the more recently formed arches have a pebbly texture, while the surfaces of older arches are relatively smooth. Figure 18 demonstrates that pebbly regions are covered by spheroidal cells (mean diameter about 8·5 μm) with randomly distributed microvilli. In smooth regions (Fig. 20) the cells are polygonal, flatter and

broader (mean diameter about 17 μm), and with the microvilli restricted to the vicinity of cell boundaries. Figure 19 demonstrates an intermediate condition where the cells have become rather flat, but still have microvilli over their entire surfaces.

Stage 17 (*Fig.* 10)

At this stage (about 10½ days) the nasal and optic placodes are deeply invaginated. The perinasal processes flair outward and downward from the frontal bulges to form a raised rim around the nasal antrum. Superiorly, the medial and lateral nasal processes are separated by a slight constriction of the rim. Inferiorly, beneath the nasal canal, the rim is flattened because here the lateral nasal process is rather flat. The maxillary process extends medially to contact the two nasal processes, and there is a lambdoid junction where the maxillo-lateral nasal groove, the maxillo-medial nasal groove and the medial nasal–lateral nasal groove meet.

Arch I (including the maxillary process) has become sickle-shaped and borders about three fourths of the stomatodeal antrum, as viewed from the side. Arch II has expanded laterally and widened so that the floor of G-1 is obscured. A slight constriction at the mid-lateral portion of II divides this arch into dorsal and ventral bulges.

The cervical sinus is reduced in size and the ventral bulge of II obscures most of G-2 and the ventral (medial) end of III. The opening of the otocyst has closed over and the glossopharyngeal placode invagination in G-2 has disappeared, but the vagus placode is now seen at the distal end of G-3 where the latter curves caudally below IV. Arch IV and G-4 have been reduced to vestiges in the form of a tag and a dimple on the cephalad-inclined surface of the epipericardial ridge.

At this stage the epithelial cells lining the cervical sinus are still spheroidal (Fig. 18), but all other visceral arch and facial surfaces have flat cells (Fig. 20).

Stage 18 (*Figs.* 11 *and* 12)

At this stage (the first half of the eleventh day) the lens vesicle is closed. The frontal aspect of the head tapers above and below its widest (1·7 mm) level, which is across the middle of the maxillary bulges. Above, it narrows to 1·5 mm at the outer borders of the lateral nasal process, while below, the head tapers to 1·4 mm at the level of I and to 1·2 mm at the level of II.

The perinasal rims (formed by the medial and lateral nasal processes) extend about 0·5 mm outward from the primary surface of the frontal bulges. The two medial nasal processes are separated by the much enlarged frontal groove (0·25 mm wide), which is now continuous with the roof of the stomatodeum. The antrum of the nasal canal has elongated (0·3 mm) and the medial nasal process is longer (0·6 mm) than the lateral nasal process (0·5 mm). The inferior ends of the medial nasal processes (globular processes) protrude further outward and downward than the other components at the lambdoidal junctions. In consequence, the groove separating the medial nasal process from the maxillary and lateral nasal process is accentuated to form a single oronasal fissure.

The sides of the stomatodeal antrum have become slit-like because the maxillary and mandibular processes are in contact here. Centrally, the antrum is a rhomboid-shaped opening: the upper margin is the frontal groove and the lower margin is the V-shaped junction where the right and left mandibular processes have united. From the frontal aspect, the maxillary process and I and II are stacked one upon the other

Table 1. *Summary of the development of external features of the face and visceral arches of the mouse embryo*

(Classified according to Theiler's (1971) developmental stages 12–21 (8–13 days *post coitum*).)

Stage 12, early

(*a*) encephalic groove open
(*b*) prosencephalon flared laterally
(*c*) primary optic vesicles are shallow concavities
(*d*) region of future visceral arch development lies between heart and brain primordia

Stage 12, late

(*a*) mid-brain elongated
(*b*) cephalic flexure present
(*c*) cervical fold formed
(*d*) future visceral arch region becomes enlarged and rectangular

Stage 13

(*a*) fore-brain at right angle to hind-brain
(*b*) primordium of arch I formed
(*c*) cervical fold enlarged and forms posterior boundary of amniotic subcompartment

Stage 14

(*a*) embryo has rotated; front of head faces 'abdomen'
(*b*) encephalic groove closed
(*c*) midsagittal ridge on frontal prominence
(*d*) nasal placode beginning
(*e*) arch I much enlarged but unfused ventrally
(*f*) arch II forming
(*g*) cervical sinus forming with primordium of III
(*h*) otic placode at lateral aspect of hind-brain above G-2
(*i*) glossopharyngeal placode forming in G-2

Stage 15

(*a*) midsagittal ridge disappears
(*b*) lateral bulges of frontal prominence enlarged
(*c*) maxillary primordium forming as lateral bulge on I
(*d*) upper margin of I is concave
(*e*) entire visceral arch region posterior to I is recessed
(*f*) arch II enlarged and G-1 and G-2 deepened
(*g*) glossopharyngeal and otic placodes form canals
(*h*) arch IV and G-4 forming
(*i*) spheroid epithelial cells begin to flatten

Stage 16

(*a*) frontal groove formed
(*b*) lateral and medial nasal processes distinct
(*c*) optic placode elevated
(*d*) maxillary process extends above stomatodeal commissure
(*e*) upper border of I becomes convex
(*f*) arch II enlarged and G-1 becomes slit-like
(*g*) cervical sinus and its structures become reduced

Stage 17

(*a*) nasal and optic placodes invaginated
(*b*) upper ends of medial and lateral nasal processes separated by constriction of perinasal rim
(*c*) distinct lambdoid junction beneath nasal antrum
(*d*) arch I (including maxillary process) surrounds three fourths of stomatodeal antrum
(*e*) arch II expanded and secondary bulges forming
(*f*) part of III obscured by II
(*g*) openings of otic and glossopharyngeal placodes obliterated
(*h*) vagus placode apparent in G-3
(*i*) arch IV and G-4 reduced to tag and dimple

Table 1. (*cont.*)

Stage 18

(*a*) lens vesicle closed
(*b*) frontal groove much enlarged and continuous with stomatodeum
(*c*) globular process and oronasal fissure formed
(*d*) nasolacrimal groove deepening
(*e*) lateral part of G-2 obliterated
(*f*) arch III vestigial
(*g*) arch IV, G-3 and G-4 obliterated
(*h*) cervical sinus is small concavity

Stage 19

(*a*) frontal groove becomes narrow fissure
(*b*) nasolacrimal groove beginning to merge medially
(*c*) primary choanae formed
(*d*) secondary tubercles forming on I and II
(*e*) external auditory meatus beginning as widened slit in G-1
(*f*) placode of facial nerve visible in lateral part of G-1
(*g*) arch III obliterated
(*h*) vagus placode forms canal
(*i*) cervical sinus area becomes cephalad incline of epipericardial ridge

Stage 20

(*a*) frontal prominence enlarged due to expansion of cerebral hemispheres
(*b*) angle between frontal prominence and perinasal structures gives a more snout-like profile
(*c*) upper lip is forming
(*d*) marked merging at lambdoid junction
(*e*) mandibular arch lies inside maxillary arch
(*f*) G-1 obliterated on either side of auditory meatus
(*g*) vagus placode opening obliterated

Stage 21

(*a*) eyes have more medial position
(*b*) frontal fissure closed
(*c*) nasolacrimal groove closed
(*d*) supraorbital tubercles formed
(*e*) vibrissae placodes appear on maxillary process
(*f*) external nares develop inverted comma shape
(*g*) mandibular process tucked between 'abdomen' and overhanging maxillary process
(*h*) arch II becoming part of neck contour
(*i*) auditory meatus is a round hole on side of neck
(*j*) former cervical region represented by wrinkle at base of neck
(*k*) end of embryonic period

with a slight upward incline toward the middle. As measured from the side, I is about 0·36 mm wide, the maxillary process is slightly narrower (0·35 mm) while II is the thinnest (0·29 mm).

Stereograms show the maxillary process to be expanded laterally with a corresponding deepening of the depression separating it from the eye and lateral nasal process (nasolacrimal groove).

The maxillary process and I and II bend at right angles from the sides toward the front (ventral). The bend of II is accentuated by its bulge at the corner. The first visceral groove (G-1) extends the full length between I and II (laterally and ventrally). In contrast, the lateral aspect of G-2 is completely obliterated, except for the incisure beneath the corner bulge where II overhangs the vestige of III. The rest of the cervical sinus remains as a small concavity with the button-like vagus placode at its centre. The entire epithelial surface is now smooth (Fig. 20).

Stage 19 (*Figs.* 13 *and* 14)

At this stage (in the second half of the eleventh day) the frontal groove has been reduced to a narrow fissure by convergence of the expanded medial nasal processes. The grooves at the lambdoid junction have become shallow and the nasolacrimal groove is beginning to close in an upward–lateral direction toward the inner canthus of the eye. The oronasal fissure is flatter, the globular processes are reduced and the nasal canals have perforated into the stomatodeum to form primary choanae just behind the lambdoid junction.

The anterior rhomboid opening of the stomatodeum has narrowed because of the reduced width of the frontal groove above, and the continued merging of the right and left mandibular processes below.

Arch I has become proportionately broader. It is also topologically more complex because three secondary tubercles have formed on either side of the ventral groove. One tubercle is lateral to the midline near the margin of G-1, another is near the stomatodeal border anterior to the commissure, and the third tubercle is behind the commissure near the base of I. Arch II has also become more complex: its overall shape is triangular with one angle adjoining the heart bulge (ventrally) another angle adjoining the epipericardial ridge (caudally) and the third angle butted against the base of I (cranio-dorsally). Four tubercles have developed on II, one at each corner of the triangle, and the fourth, (largest) in the centre next to G-1.

The beginning of the formation of the external auditory meatus is indicated by a widening of the ventral aspect of G-1. A smaller widening dorsally indicates the location of the facial nerve placode.

The cervical sinus has become reduced still further: it is now a simple triangular area lying below, and partly tucked under, II. The two branchial arches (III and IV) are now completely obliterated as such, and only the deeply invaginated vagus placode occupies the centre of the sinus. The superior boundary of the cervical sinus appears to be sharply defined by G-2 in lateral view (Fig. 14), but from a more ventral aspect (Fig. 13) it is seen as the inclined surface of the epipericardial ridge, with no sharp separation from II.

Stage 20 (*Figs.* 15 *and* 16)

At this stage (the twelfth day) the frontal prominence is much enlarged as a result of the growth of the cerebral hemispheres. This causes the combined nasal and maxillary processes to protrude at a more acute angle, and to appear more snout-like in profile. The superior margin of the stomatodeum is beginning to resemble a lip because of the increased overhang of the maxillary process laterally and a deepening of the vault centrally. The latter is related to the reduction of the frontal groove (fissure) and to continued merging of the globular and maxillary processes. Merging has also progressed of all the other components at the lambdoid junction.

The mandibular process is still wider (0·5 mm) than the maxillary process, but it conforms to the arc of a smaller circle, and therefore lies within the arch of the superior margin of the stomatodeum. The latter is formed by the maxillary and medial nasal processes. Medially, the V-shaped groove has become shallow at the stomatodeal border of I, but it is still deeply invaginated along the line of merging on the ventral surface.

Arches I and II have begun to merge on either side of the auditory meatus, but the obliteration of G-1 is more advanced laterally. However, the facial nerve

placode is still present as a dimple near the lateral extremity of G-1. The tubercles on II have expanded and are more distinct. The lateral–inferior base of this arch is now completely continuous with the epipericardial ridge, the result of merging at the lateral part of G-2. The cervical sinus is now represented by the small triangular cephalo-medial slope of the epipericardial ridge as it joins the surface of the heart bulge. The vagus placode is no longer visible.

Stage 21 (*Fig.* 17)

Now (the thirteenth day) the eyes have assumed a more medial position, supra-orbital tubercles have formed and the basic features of the mouse face are established. The frontal fissure has closed and only a slight midsagittal depression remains. The nasal-lacrimal fissure has also closed, and thus the union of maxillary process with lateral nasal process is complete except for a slight longitudinal indentation. The medial region of the maxillary process dominates the side of the face: its labial portion completely obscures I ventrally; its infraorbital portion rises above the margin of the eye at the periorbital groove, and the fronto-lateral surface is covered with raised primordia of vibrissae.

The external nares have assumed their characteristic inverted comma shape as the result of positional readjustment between the lateral and medial nasal processes.

Viewed from the front, the mandibular arch is completely obscured by the over-hanging maxillary process above and the abdominal bulge below. Viewed from the side, G-1 is obliterated on both sides of the auditory meatus, which has become enlarged and circular. Except for this space, merging of I and II is now completed. The medial aspect of II forms the incipient neck contour below I, while the lateral aspect of II, below the primordia of the external ear, joins the cervical sinus area which has become a lateral wrinkle at the base of the neck.

From an epigenetic standpoint the embryonic phase is now essentially concluded and later development *in utero* is in the fetal phase.

Table 1 is a résumé of the main points brought out in this report.

DISCUSSION

There is always the risk of error when giving a longitudinal interpretation to cross sectional data. But, obviously, it is not possible to follow the continuous development of a single specimen under conditions that are compatible with life. Longitudinal studies of embryos grown *in vitro* (Tamarin & Jones, 1968) might provide data with which cross sectional observations could be compared; but unfortunately *in vitro* morphogenesis tends to be abnormal. A more basic constraint on the feasibility of longitudinal studies at high magnification is the relatively limited resolution of incident-light microscopy. On the other hand, variation in the degree of development within a single litter is a fortunate circumstance for a cross sectional study. The large number of specimens used here allowed for at least six samples in any 24 hour period. Thereafter, a cautious extrapolation of 'continuous change' from these cross sectional data does not seem unreasonable.

Although the first visceral arch is the first definitive facial structure to form, the prior formation of the cervical fold may be an essential, though impermanent, component of face and neck development. The cervical fold seems to be the progenitor of the epipericardial ridge, and establishes the posterior boundary of the visceral arch region. Since it forms before the rotation of the embryo, the cervical fold may

also serve the transitory function of keeping the amnion from impinging on facial primordia as the embryo's posture changes. Since Witschi's (1956) brief reference to it, the cervical fold in mammals appears to have been a neglected topic until recently (Tamarin & Boyde, 1976). Our present findings on this structure are suggestive rather than definitive, and the subject deserves further study.

Our observations do not support the notion that the hyoid arch forms an operculum which overgrows and obliterates the cervical sinus and its constituent structures. The visceral arches differentiate in a cephalo-caudal sequence and then are obliterated in reverse order. Thus arch IV, which has a very brief existence (about 36 hours), disappears as a surface structure at a time when the separation of II from III by G-2 is still very distinct. As II widens, its lower edge tends partly to overhang III, but there is no evidence that II fuses with structures lying beyond III. With appropriate tilting of the specimen, and with stereoscopic observation (Figs. 11 and 12), the regression of III is seen to occur independently of and prior to the obliteration of G-2. From these findings it would seem that many textbook accounts of cervical sinus involution need to be revised. However, our observations do not conflict with Frazer's (1926) general description, nor with Garrett's (1948) corroborative report on the cervical sinus in human embryos.

Placodes of the cranial nerve (7–10) sensory ganglia occur in positional association with the visceral grooves, as predicted by comparative anatomical studies in lower vertebrates (Goodrich, 1918). But here our findings differ slightly from Frazer's (1926). We find no evidence that the vagus placode canal is obliterated by IV: on the contrary, the placode antrum is still present after IV disappears.

Development of the upper face in mice appears to differ from human facial development in at least two important respects. In mice, the fronto-lateral expansions of the frontal prominence create two bulges separated by a midsagittal groove prior to the appearance of the nasal placodes and the paranasal processes; in man, the midsagittal groove results secondarily from the enlargement of the medial nasal processes (Patten, 1961). Thus, in the mouse, the frontal groove develops relatively earlier and forms a more profound division between the right and left halves of the face; in man the right–left division is of relatively short duration and, basically, the structures which occur between the two maxillary processes appear to develop as a single unit (the intermaxillary segment) with no separation at the upper central border of the stomatodeum.

Another, but less profound, difference between the two species lies in certain details of the relationship between the maxillary process and its neighbouring structures at the lambdoid junction. When the lambdoid junction of the mouse is viewed from the front, the zone of contact between the maxillary process and the medial nasal process appears proportionately narrower than its contact with the lateral nasal process. This relationship appears reversed in man; i.e. contact with the medial nasal process is proportionately wider (based on subjective impressions of photographs of human embryos of appropriate developmental age), and this seems to affect the geometry of the globular process and oronasal fissure.

Differences as well as similarities, must be kept in mind when extrapolating the events of mouse development to man: it is hoped that this report will be of use in the task of establishing such differences and similarities.

SUMMARY

The morphogenesis of the face and visceral arch region were studied by scanning electron microscopy in 63 mouse embryos between 8 and 13 days *post coitum*. The developmental stages were determined by reference to Theiler's (1971) scheme for the categorization of the normal stages of development.

After the cervical fold is formed (stage 12) the mandibular primordium appears (stage 13) followed by the primordia of arches II and III (stage 14) with arch IV forming last (stage 15). Arches II, III and IV regress in reverse order, with *no evidence that a cervical sinus pouch is formed.* Placodes of the sensory ganglia from cranial nerves 7, 9 and 10 are formed in the first, second and third visceral grooves respectively. Formation of the external auditory meatus and its surrounding tubercles were also observed.

Morphogenesis of the upper face is dominated by the midsagittal groove, which extends into the stomatodeum; and by the medial nasal, lateral nasal and maxillary processes. The temporal changes in shape and the interrelationships of the structures mentioned are described in detail.

We are grateful to Elaine Bailey for help in the laboratory at University College London and to Dr Anne McLaren and Kathy Ellis at the Medical Research Council's Mammalian Development Unit for providing the accurately timed pregnant mice used in this study. This study was supported, in part, by a Fogerty International Senior Research Fellowship awarded to the senior author.

REFERENCES

BALFOUR, F. M. (1878). Monograph on the development of elasmobranch fishes. In *The Works of Francis Maitland Balfour* (1885), vol 1 (ed. M. Foster and A. Sedgwick). London: Macmillan and Co.

BARRY, A. (1961). Development of the branchial region of human embryos with special reference to the fate of epithelia. In *Congenital Anomalies of the Face and Associated Structures* (ed. S. Pruzansky). Springfield: C. Thomas.

BOYDE, A., JONES, S. J. & BAILEY, E. (1973). Bibliography on Biomedical Applications of SEM. *Scanning Electron Microscopy*/1973 (ed. O. Johari and I. Corvin), pp. 697–734. Chicago: Illinois Institute of Technology Research Institute.

BOYDE, A., BAILEY, E., JONES, S. J. & TAMARIN A. (1977). Dimensional changes during specimen preparation for scanning electron microscopy. *Scanning Electron Microscopy*, Vol. 1 (ed. O. Johari and R. Becker) pp. 507-518. Chicago: Illinois Institute of Technology Research Institute.

BURLINGHAME, P. L. & LONG, J. A. (1939). The development of the external form of the rat, with some observations on the origin of the extraembryonic coelom and foetal membranes. *California University Publications in Zoology* **43**, 143–336.

CADENAT, M. E. (1961). Embryology of the mouth and face. *Plastic and Reconstructive Surgery* **28**, 329-336.

CHRISTIE, G. A. (1964). Developmental stages in somite and post-somite rat embryos, based on external appearance, and including some features of the macroscopic development of the oral cavity. *Journal of Morphology* **114**, 263–286.

FRAZER, J. E. (1926). The disappearance of the precervical sinus. *Journal of Anatomy* **61**, 132–143.

GARRETT, F. D. (1948). Development of the cervical vesicles in man. *Anatomical Record* **100**, 101–113.

GOODRICH, E. S. (1918). On the development of the segments of the head of *Scyllium*. *Quarterly Journal of Microscopical Science* **63**, 1–30.

GRÜNEBERG, H. (1943). The development of some external features in mouse embryos. *Journal of Heredity* **34**, 88–92.

HIS, W. (1866). Ueber der Sinus praecervicalis über die Thymusanlage. *Archiv für Anatomie und Physiologie, Anatomische Abteilung.*

JOHNSON, V. E. (1976). The scanning electron microscope in biology: a bibliography. *Scanning Electron Microscopy*/1976 (ed. O. Johari and R. P. Becker), pp. 637–701. Chicago: Illinois Institute of Technology Research Institute.

JONES, S. J., BAILEY, E. & BOYDE, A. (1974). Biomedical applications bibliography, 1973–74, update. *Scanning Electron Microscopy*/1974 (ed. O. Johari and I. Corvin) pp. 835–850. Chicago: Illinois Institute of Technology Research Institute.

KINGSBURY, B. F. (1926). Branchiomerism and the theory of head segmentation. *Journal of Morphology* **42**, 83–109.

KIRBY, D. R. S. (1971). The transplantation of mouse eggs and trophoblasts to extrauterine sites. In *Methods in Mammalian Embryology* (ed. J. C. Daniel, Jr), pp. 146–156. San Francisco: W. H. Freeman and Co.

LOCY, W. A. (1895). Contribution to the structure and development of the vertebrate head. *Journal of Morphology* **11**, 497–594.

NELSEN, O. E. (1953). *Comparative Embryology of the Vertebrates*. New York: Blakiston Co.

OTIS, E. M. & BRENT, R. (1959). Equivalent ages in mouse and human embryos. *Anatomical Record* **120**, 33–64.

OWEN, R. (1848). *On the Archetype and Homologies of the Vetebrate Skeleton*. London: John Van Voorst.

PATTEN, B. M. (1961). The normal development of the facial region. In *Congenital Anomalies of the Face and Associated Structures*, (ed. S. Pruzansky), pp. 11–45. Springfield: C. Thomas.

RUGH, R. (1968). *The Mouse: Its Reproduction and Development*. Minneapolis: Burgess Publishing Co.

STREETER, G. L. (1942). Developmental horizons in human embryos. *Contributions to Embryology* **30**, 211–245.

STREETER, G. L. (1948). Developmental horizons in human embryos. *Contributions to Embryology* **32**, 27–63.

SUDLER, M. T. (1902). The development of the nose and of the pharynx and its derivatives in man. *American Journal of Anatomy* **1**, 391–416.

TAMARIN, A. & JONES, K. (1968). A circulating medium system permitting manipulation during culture of postimplantation embryos. *Acta embryologica et morphologica* **10**, 288–301.

TAMARIN, A. & BOYDE, A. (1976). Three-dimensional anatomy of the eight-day mouse conceptus: a study by scanning electron microscopy. *Journal of Embryology and Experimental Morphology*. **36**, 575-596.

THEILER, K. (1971). *The House Mouse: Development and Normal Stages from Fertilization to Four Weeks of Age*. New York: Springer Verlag.

WATERMAN, R. E. (1974*a*). SEM studies of early facial development in rodents and man. *Scanning Electron Microscopy*/1974, (ed. O. Johari and I. Corvin), pp. 533–540. Chicago: Illinois Institute of Technology Research Institute.

WATERMAN, R. E. (1974*b*). Embryonic and foetal tissues of vertebrates. In *Principles and Techniques of Scanning Electron Microscopy*, vol. 2 (ed. M. A. Hayat). pp. 93–110. New York: Van Nostrand Reinhold Co.

WATSON, J. H. L., ASFARI, A., DRUKKER, B. H. & SWEDO, J. L. (1976). Scanning electron microscopy of human embryos, in *Scanning Electron Microscopy*/1976/*II* (ed. O. Johari and R. P. Becker), pp. 394–399. Chicago: Illinois Institute of Technology Research Institute.

WEDIN, B. (1954). Proneuromeres and neuromeres in the cerebral tube of *torpedo ocellato*. *Acta anatomica* **21**, 59–69.

WITSCHI, E. (1956). *Development of Vertebrates. London*: W. S. Saunders Co.